

INTERNATIONAL SOCIETY FOR SOIL MECHANICS AND GEOTECHNICAL ENGINEERING



This paper was downloaded from the Online Library of the International Society for Soil Mechanics and Geotechnical Engineering (ISSMGE). The library is available here:

<https://www.issmge.org/publications/online-library>

This is an open-access database that archives thousands of papers published under the Auspices of the ISSMGE and maintained by the Innovation and Development Committee of ISSMGE.

The paper was published in the proceedings of the 20th International Conference on Soil Mechanics and Geotechnical Engineering and was edited by Mizanur Rahman and Mark Jaksa. The conference was held from May 1st to May 5th 2022 in Sydney, Australia.

Lateral spreading force to pile foundation on liquefiable slope

Force de propagation latérale à la fondation sur pieux sur une pente liquéfiable

Byeong-Soo Yoo & Kyo-Young Gu & Nghiem Xuan Tran & Sung-Ryul Kim

Dept. of Civil and Environmental Eng., Seoul National Univ., South Korea, ybspnut@snu.ac.kr

Mintaek Yoo

Railroad structure research team, Korea railroad research institute, South Korea

ABSTRACT: Liquefaction-induced lateral force is one of the significant considerations in the seismic design of piles. In this study, the effects of stiff slope on the lateral force were examined by performing a centrifuge test. The pile-deck system was embedded in the saturated loose sandy ground with an inclination of 27° . The model was excited at the container base by a ramped sinusoidal wave of 1.5 Hz frequency. Test results show that the non-liquefied soil above the slope toe substantially pushes the piles toward the downslope considering the liquefaction occurrence below the slope toe. The maximum bending moment of the piles appears at the pile toe induced by kinematic force as the lateral spreading occurred. The experimental lateral forces derived from the peak monotonic bending moment are concentrated near the slope toe. The concentrated lateral forces are compared with those calculated by conventional suggestions for piles in a horizontal ground or gentle slope. The concentrated lateral forces on piles in slope are larger and smaller than those on piles in the liquefied layer and in the non-liquefiable crust, respectively. Therefore, the ground above the slope toe should be considered as a non-liquefiable crust in the seismic design of piles even though it is loose-saturated sand.

RÉSUMÉ : La force latérale induite par la liquéfaction est l'une des considérations importantes dans la conception sismique des pieux. Dans cette étude, les effets d'une pente raide sur la force latérale ont été examinés en effectuant un test de centrifugation. Le système de pieux-deck a été enfoncé dans le sol sablonneux lâche saturé avec une inclinaison de 27° . Le modèle a été excité à la base du conteneur par une onde sinusoïdale en rampe de fréquence 1,5 Hz. Les résultats des tests montrent que le sol non liquéfié au-dessus du pied de pente pousse sensiblement les pieux vers le bas de la pente compte tenu de l'occurrence de liquéfaction sous le pied de pente. Le moment de flexion maximal des pieux apparaît au pied du pieux induit par la force cinématique lors de l'étalement latéral. Les forces latérales expérimentales dérivées du moment de flexion monotone maximal sont concentrées près du pied de pente. Les efforts latéraux concentrés sont comparés à ceux calculés par des suggestions conventionnelles pour des pieux en terrain horizontal ou en pente douce. Les forces latérales concentrées sur les pieux en pente sont plus grandes et plus petites que celles sur les pieux dans la couche liquéfiée et dans la croûte non liquéfiable, respectivement. Par conséquent, le sol au-dessus du pied de talus doit être considéré comme une croûte non liquéfiable dans la conception sismique des pieux, même s'il s'agit de sable lâche saturé.

KEYWORDS: liquefaction-induced lateral force; slope; laterally loaded pile; liquefaction; centrifuge test.

1 INTRODUCTION

Lateral spreading induced by ground liquefaction has caused considerable damage to pile foundations (Hamada and O'Rourke 1992, Youd 1993, Berrill, Christensen et al. 2001, PIANC 2001). A substantial kinematic force by the lateral spreading of the ground is applied to the pile when liquefaction occurs. Consequently, several methods to calculate the force induced by the lateral spreading of a horizontal ground or gentle slope has been proposed on the basis of data obtained from case histories and experiments.

The force induced by a liquefied layer has been proposed to be proportional to the total stress of the ground (JSWA 1997, He, Elgamal et al. 2009, JRA 2012), or uniform (Dobry, Abdoun et al. 2003, González, Abdoun et al. 2009, Chiou, Huang et al. 2021). JRA (2012) proposed that the lateral force is 30% of the division of the total stress times the outermost width of the group by the number of piles in the group. JSWA (1997) suggested 50% of the total stress times the pile diameter. He, Elgamal et al. (2009) found that the lateral pressure applied on the pile diameter is the same as the total stress which is the hydrostatic pressure of a fluid with a saturated unit weight of the liquefied soil. Dobry, Abdoun et al. (2003) suggested that a uniform lateral load in the liquefied layer is approximately 10 kPa times the pile diameter. González, Abdoun et al. (2009) found that the uniform lateral forces are 11.5 and 8.3 kPa times the pile diameter by the centrifuge tests on single and group piles. Chiou, Huang et al.

(2021) found that the uniform lateral forces are 3.4 and 4.2 kPa times the pile diameter by the shaking table tests on soft and stiff piles, respectively.

The force induced by a non-liquefiable crust, which is normally a sand layer above the groundwater table or a clay layer, overlying a liquefied layer has been proposed based on the passive earth pressure. JRA (2012) proposed that the lateral force is passive earth pressure times the outermost width of the group by the number of piles in the group with a correction factor considering the level of liquefaction by liquefaction potential index (LPI). Cubrinovski, Kokusho et al. (2006) suggested that the lateral force is the Rankine passive earth pressure times pile diameter with a shape factor of 4.5. Cubrinovski, Ishihara et al. (2009) commented that pile-group effects reduce the lateral force. Chiou, Huang et al. (2021) found that the lateral forces are 4.5 times the Rankine passive earth pressure with the pile diameter and 3 times the Coulomb passive earth pressure with pile diameter.

The piles damaged by liquefaction-induced lateral spreading were mainly a foundations of waterfront structures. The natural ground formed by sedimentation at such areas, which is susceptible to liquefaction-induced lateral spreading, usually has a slope angle of 15° – 30° . The lateral spreading of the slope can be encouraged by the liquefied layer below the slope. McCullough, Dickenson et al. (2001) conducted a series of centrifuge tests on the pile-supported wharf in a sloping rock-fill overlying a liquefiable layer. The model pile was suffered by

large bending moment induced by the lateral spreading of the slope despite the loose sand layer was not fully liquefied. This soil movement might cause a considerable lateral force on pile, especially under full liquefaction (Boulanger, Kutter et al. 2003). Souri, Khosravifar et al. (2018) found that the maximum bending moment induced by the kinematic load of lateral spreading occurs at the top and the bottom of the liquefiable layer by analyzing the data provided by McCullough, Dickenson et al. (2001). Saha, Horikoshi et al. (2020) reported that the resultant earth pressure of the sheet pile in the sloping embankment overlying liquefiable layer is maximum at the middle of the liquefiable layer, which is different from the suggestions of JRA (2012), JSWA (1997), and He, Elgamal et al. (2009).

The lateral flow of the stiff slope mainly occurs above the slope toe rather than in the entire liquefied layer unlike the case of horizontal ground. Therefore, the lateral forces distributed along the pile in the sloping ground might be considerably different from those of the horizontal ground. Few previous experiments were performed on piles in the ground with stiff slope. Research is still needed to improve the current understanding and to provide appropriate recommendations for practical designs.

This study aims to improve the understanding of the dynamic behavior of pile foundations embedded in a stiff slope under liquefaction triggering by performing a centrifuge model test. The dynamic centrifuge model test was conducted on single and group piles in a 27° sloping ground. The overall seismic behavior of the model ground and pile was analyzed in terms of the measured pore pressure, settlement of the ground, and the bending moment of the piles. The experimental lateral force on piles induced by the liquefaction triggering was derived from the monotonic component of the measured bending moment. A detail discussion on the current seismic designs of pile foundations in the liquefied ground was made.

2 CENTRIFUGE MODELING

Beam-type geotechnical centrifuge equipment with a 5 m radius was employed for the centrifuge test at the Korea Advanced Institute and Science Technology. The maximum capacity of the equipment is 240 g-t. The test model was built in an equivalent shear beam (ESB) cube-shaped container with a length of 65 cm to minimize the boundary effect (Lee, Choo et al. 2013).

Figure 1 shows the layout of the centrifuge test model. The model structures were two decks supported by a 2×2 pile group and a single pile. It was simulated by applying a length scale factor of 34 to the pile-supported wharf in Pohang New Port, Korea. The dimensions of the model structure were determined in accordance with the scaling law of Madabhushi (2014). The dimension of the model pile was determined on the basis of the scale of flexural stiffness to adequately simulate the response of the pile to the horizontal load. The flexural stiffness of the model pile was $8.42 \times 10^5 \text{ kN} \cdot \text{m}^2$. The model pile was 0.85 m in diameter, 0.07 m in thickness, and 18 m in length. The dimension of the model deck was determined on the basis of the weight of the super-structure. The deck on group piles was 4 times heavier than that on the single pile. Pile response was measured with strain gauges attached to the piles.

The model ground was saturated loose silica sand with a stiff inclination of 27°. The relative density and saturated unit weight were 35% and 18 kN/m^3 , respectively. Table 1 shows the properties of silica sand used in this study. Ground response was measured with pore pressure transducers (PPTs) and linear variable differential transformers (LVDTs). Pore pressure was measured by inserting PPTs behind the crest. PPTs were attached to the thin steel bar so that the location of PPTs was fixed even in the case of ground deformation. Two LVDTs were placed behind the crest to measure the ground settlement.

The experimental model was constructed in the following order. First, the thin steel bar with PPTs and the model piles with strain gauges were fixed on the container base. Second, the container was filled with water, and the model ground was formed by pluviating the saturated silica sand through a sieve. Third, the slope surface was manually created after lowering the water level. The decks were then rigidly connected to the pile heads followed by the installation of the LVDTs. Subsequently, the test model was spun up to the target centrifuge acceleration, and the miniature cone penetration test was performed to determine the properties of the model ground (Kim, Choo et al. 2016). Finally, a ramped sine wave with a maximum acceleration of 0.25 g and a frequency of 1.5 Hz was applied at the container base, as shown in Fig. 2.

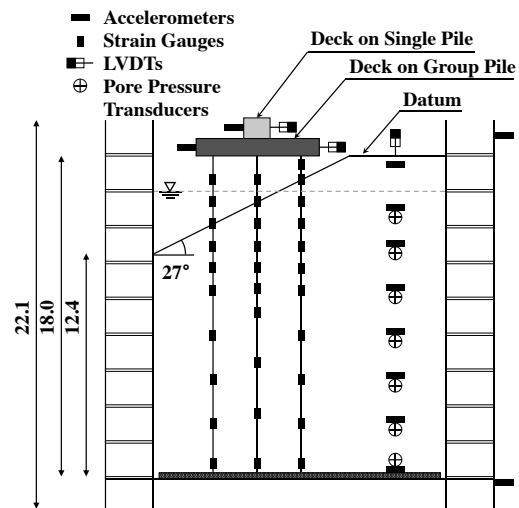


Figure 1. Layout of centrifuge test model (unit: m)

Table 1. Soil properties of silica sand

Properties	Values
Relative density D_r (%)	35
Specific gravity G_s	2.65
Saturated unit weight γ_{sat} (kN/m^3)	18.0
Max. dry unit weight $\gamma_{d(max)}$ (kN/m^3)	16.1
Min. dry unit weight $\gamma_{d(min)}$ (kN/m^3)	12.2
	$D_{10} = 0.148$
Grain size (mm)	$D_{50} = 0.237$
	$D_{60} = 0.257$
Uniformity coefficient C_u	1.60
Soil classification (USCS)	SP

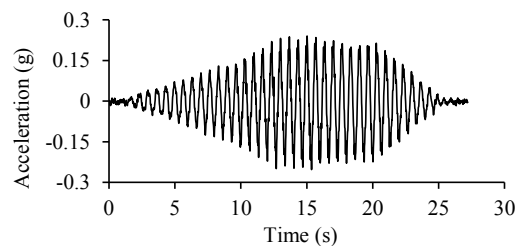


Figure 2. Input acceleration time history

3 EXPERIMENTAL LATERAL SPREADING FORCE

Considering the pile subjected to seismic load in the sloping ground, the time history of the measured bending moment consisted of the transient component generated by the structural mass and the monotonic component induced by the lateral spreading. Moreover, the monotonic component has a great proportion of the measured bending moment considering the liquefaction triggering (Abdoun and Dobry 2002). The monotonic component was extracted from the measured bending moment by Fast Fourier transform smoothing with a cutoff frequency of 0.5 Hz. The transient component was calculated by subtracting the monotonic component from the measured bending moment.

The experimental lateral force acting on the pile can be determined on the basis of the second-order derivative of the monotonic bending moment profile given by Eq. 1. The experimental lateral force can be interpreted as the load and the resistance if it is positive and negative, respectively.

$$P(z) = \frac{d^2}{dz^2} M_{mono}(z) \quad (1)$$

Where, P is the lateral force, M_{mono} is the monotonic bending moment, z is the distance from the pile head.

A cubic spline method was adopted to fit the monotonic bending moment profile below the ground surface as shown in Eq. 2. Haiderali and Madabhushi (2016) suggested that cubic spline method is suitable to derive the mobilized soil pressure for the laterally loaded piles. The second derivative of the monotonic bending moment at the ground surface was assumed to be zero in accordance with Eq. 3, and the boundary condition at the pile toe was restrained to reflect the centrifuge test. The continuities of the bending moment, shear, and lateral force were ensured by using Eqs. 4, 5, and 6.

$$M_{mono,i}(z) = \alpha_i + \beta_i z + \lambda_i z^2 + \kappa_i z^3, \quad (\kappa_i \neq 0, \quad z_i \leq z \leq z_{i+1}, \quad i = 0, \dots, n-1) \quad (2)$$

$$M''_{mono,0}(z_0) = 0 \quad (3)$$

$$M_{mono,i}(z_{i+1}) = M_{mono,i+1}(z_{i+1}), \quad (i = 0, \dots, n-2), \quad (4)$$

$$M'_{mono,i}(z_{i+1}) = M'_{mono,i+1}(z_{i+1}), \quad (i = 0, \dots, n-2), \quad (5)$$

$$M''_{mono,i}(z_{i+1}) = M''_{mono,i+1}(z_{i+1}), \quad (i = 0, \dots, n-2), \quad (6)$$

where $M_{mono,i}(z)$ is the fitted monotonic bending moment profile; α, β, λ , and κ are the coefficients of the cubic spline function; z_i is the distance from the pile head at the measurement point i (z_0 : ground surface, z_n : pile toe); n is the number of measurement points below the ground surface; $M_{mono,i}$ is the measured monotonic bending moment at z_i .

4 TEST RESULT AND ANALYSES

4.1 Ground response

Liquefaction occurrence of the ground was examined by excess pore pressure ratio (r_u). Figure 3 shows r_u profiles along the depth at several time instants. The increase of r_u showed different trend above and below the slope toe. The r_u value below the slope toe rapidly increased to approximately 0.8, whereas it was relatively small above the slope toe. Thus, the liquefaction might occur below the slope toe only although the entire model ground was loose saturated sand.

The liquefaction-induced lateral soil movement was indirectly measured by the settlement of the ground behind the

slope crest, as shown in Fig. 4. The settlement gradually increased during shaking and exceeded the measurement limit at about 24 s. Since the r_u was maintained before the settlement reached the limit (see Fig. 3), the settlement was induced by lateral spreading rather than by consolidation of liquefied ground. Thus, the slope might gradually spread without a sudden collapse.

4.2 Pile response

Figure 5 shows the monotonic and transient components of peak bending moment for the single pile. The peak bending moment increased along with the distance from the pile head and the maximum appeared at the pile toe. The proportion of monotonic components continued to increase from the pile head to the pile toe, reaching 91% at the pile toe. Thus, the kinematic force had a dominant effect on the pile response.

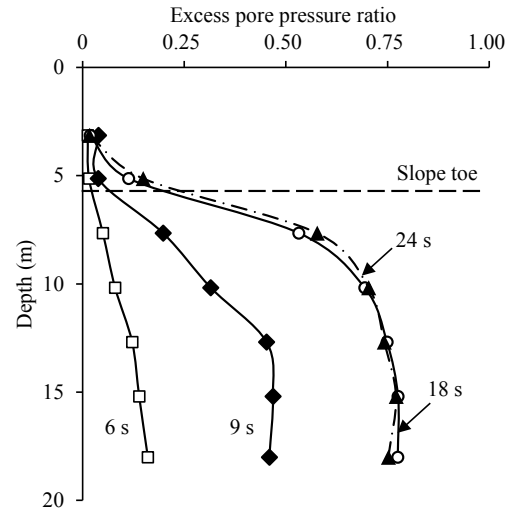


Figure 3. Excess pore pressure ratio profile

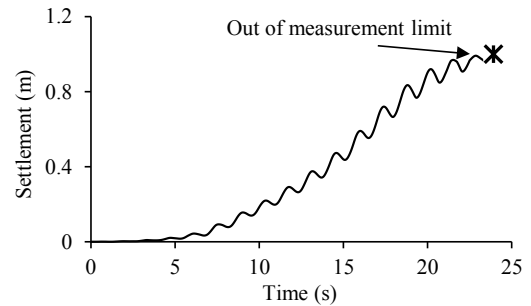


Figure 4. Time history of ground settlement behind slope crest

Moreover, the monotonic and transient bending moments did not occur at the same time (Figs. 6a and 6b). Near the ground surface, the peak transient component appeared early at approximately 6 s, indicating an insignificant reduction in soil stiffness due to a small increase in r_u . The peak monotonic component at the pile toe occurred close to the time of the maximum r_u (11 s). This observation was due to the occurrence of the lateral spreading when the ground below the slope toe was liquefied. JRA (2012) suggested to consider the liquefaction-induced lateral force and inertia force independently in the seismic design of the bridge foundation.

Figure 7 shows the experimental lateral forces to single and group piles at peak bending moment. The experimental lateral force was concentrated near the slope toe. The maximum value of the experimental lateral force of the group pile at the upslope side was approximately 3.5 times and 2.1 times larger than that of the group pile at the downslope side and the single pile, respectively. The experimental lateral force below about a 9 m

distance relative to the pile head was negative. This negative force might be attributed to an effect of the model container which prevented the flow of liquefied layer.

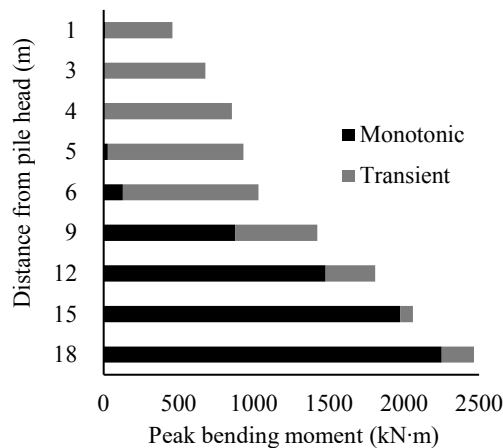


Figure 5. Proportion of monotonic and transient components of peak bending moment along the length of single pile

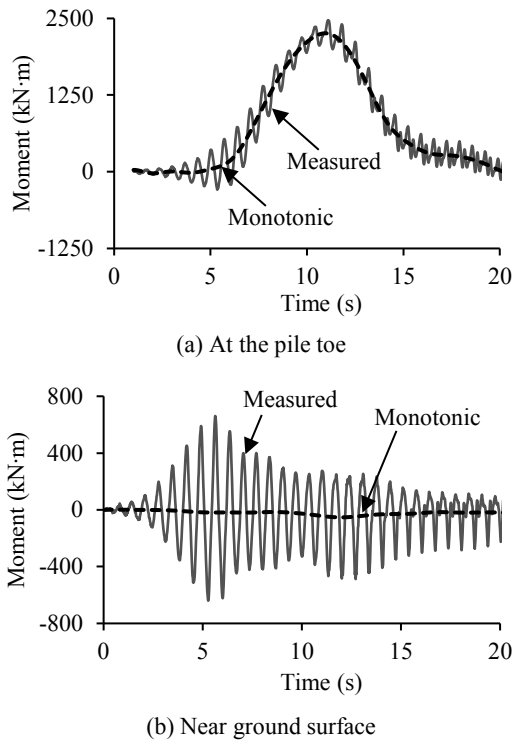


Figure 6. Effects of kinematic and inertial forces on bending moment of single pile at different distances relative to the pile head

Figure 8 shows the concentration portion of the experimental lateral force to the single pile of this study in comparison with those suggested by conventional methods. This study considered piles in the uniform sloping ground without non-liquefiable crust, whereas the conventional methods suggested a calculation procedure for the piles in a horizontal liquefied layer overlain by the non-liquefiable crust. The concentrated lateral force of this study bounded by those suggested for piles in the liquefied layer and in the non-liquefiable crust. The maximum lateral forces of the single pile and group pile at the downslope side were close to the suggestion of JRA (2012) for the non-liquefiable crust, whereas that of the group pile at the upslope side was close to the suggestion of He, Elgamal et al. (2009) for liquefied layer.

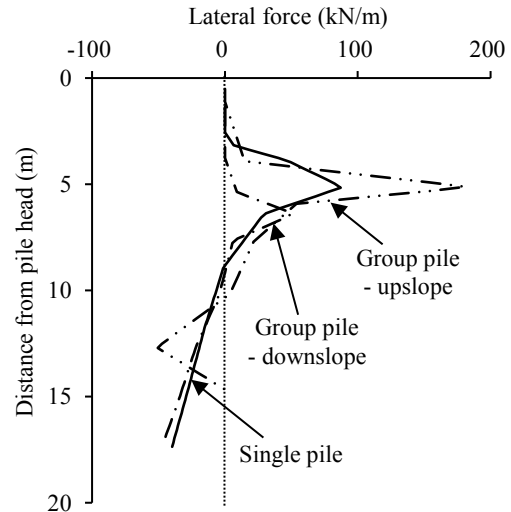


Figure 7. Experimental lateral forces at peak bending moment

5 CONCLUSIONS

The seismic response of the single and group piles on the liquefiable sloping ground was examined by a centrifuge model test. Two pile-deck systems were excited at the base with a ramped sinusoidal wave of 1.5 Hz frequency. Centrifuge test results showed that the ground above the slope toe was not liquefied, and the liquefaction occurred below the slope toe. The kinematic force due to the downslope movement of the non-liquefied soil showed a dominant effect on the pile response as the bending moment consisted of a substantial monotonic component. The experimental lateral force derived from the monotonic bending moment was concentrated near the slope toe. The concentrated lateral force to a pile in slope was larger and smaller than that in the liquefied layer and in the non-liquefiable crust, respectively. Therefore, the ground above the slope toe should be considered as a non-liquefiable crust in the seismic design of piles even though it is loose-saturated sandy soil.

6 ACKNOWLEDGEMENTS

This research was supported by the project entitled 'Development of performance-based seismic design technologies for advancement in design codes for port structures' funded by the Ministry of Oceans and Fisheries of Korea and a grant (21SCIP-C155167-03: MT21027) from Construction Technologies Program funded by Ministry of Land, Infrastructure and Transport of Korean government.

7 REFERENCES

- Abdoun, T. and R. Dobry. (2002). "Evaluation of pile foundation response to lateral spreading." *Soil Dynamics and Earthquake Engineering* 22(9-12): 1051-1058.
- Berrill, J., et al. (2001). "Case study of lateral spreading forces on a piled foundation." *Geotechnique* 51(6): 501-517.
- Boulanger, R. W., et al. (2003). *Pile foundations in liquefied and laterally spreading ground during earthquakes: centrifuge experiments & analyses*, Center for Geotechnical Modeling, Department of Civil and Environmental Engineering.
- Chiou, J.-S., et al. (2021). "Shaking table testing of two single piles of different stiffnesses subjected to liquefaction-induced lateral spreading." *Engineering Geology* 281: 105956.
- Cubrinovski, M., et al. (2006). "Interpretation from large-scale shake table tests on piles undergoing lateral spreading in liquefied soils." *Soil Dynamics and Earthquake Engineering* 26(2-4): 275-286.

Cubrinovski, M., et al. (2009). "Pseudo-static analysis of piles subjected to lateral spreading." *Bulletin of the New Zealand Society for Earthquake Engineering* 42(1): 28-38.

Dobry, R., et al. (2003). "Single piles in lateral spreads: Field bending moment evaluation." *Journal of Geotechnical and Geoenvironmental Engineering* 129(10): 879-889.

González, L., et al. (2009). "Effect of soil permeability on centrifuge modeling of pile response to lateral spreading." *Journal of Geotechnical and Geoenvironmental Engineering* 135(1): 62-73.

Haiderali, A. E. and G. Madabhushi (2016). "Evaluation of Curve Fitting Techniques in Deriving p-y Curves for Laterally Loaded Piles." *Geotechnical and Geological Engineering* 34(5): 1453-1473.

Hamada, M. and T. O'Rourke (1992). 'Case studies of liquefaction and lifeline performance during past earthquakes. Volume 1, Japanese Case Studies. Technical Rep. NCEER-92. 1: 1-28.

He, L., et al. (2009). "Liquefaction-induced lateral load on pile in a medium Dr Sand layer." *Journal of Earthquake Engineering* 13(7): 916-938.

JRA (2012). Specifications for highway bridges, Part V. Earthquake resistant design, Japan Road Association. 228.

JSWA (1997). Seismic countermeasure guidelines for sewage facilities, Japan Sewage Works Association.

Kim, J. H., et al. (2016). "Miniature Cone Tip Resistance on Sand in a Centrifuge." *Journal of Geotechnical and Geoenvironmental Engineering* 142(3).

Lee, S.-H., et al. (2013). "Performance of an equivalent shear beam (ESB) model container for dynamic geotechnical centrifuge tests." *Soil Dynamics and Earthquake Engineering* 44: 102-114.

Madabhushi, G. (2014). Centrifuge modelling for civil engineers, CRC Press.

McCullough, N. J., et al. (2001). The seismic performance of piles in waterfront applications. Ports' 01: America's Ports: Gateway to the Global Economy: 1-10.

PIANC (2001). Seismic Design Guidelines for Port Structures. Working Group, Permanent International Navigation Association.

Saha, P., et al. (2020). "Performance of sheet pile to mitigate liquefaction-induced lateral spreading of loose soil layer under the embankment." *Soil Dynamics and Earthquake Engineering* 139: 106410.

Souri, M., et al. (2018). Inertial and liquefaction-induced kinematic demands on a pile-supported Wharf: Physical modeling. *Geotechnical Earthquake Engineering and Soil Dynamics V: Numerical Modeling and Soil Structure Interaction*, American Society of Civil Engineers Reston, VA: 388-397.

Youd, T. L. (1993). "Liquefaction-induced damage to bridges." *Transportation Research Record* 1411: 35-41.

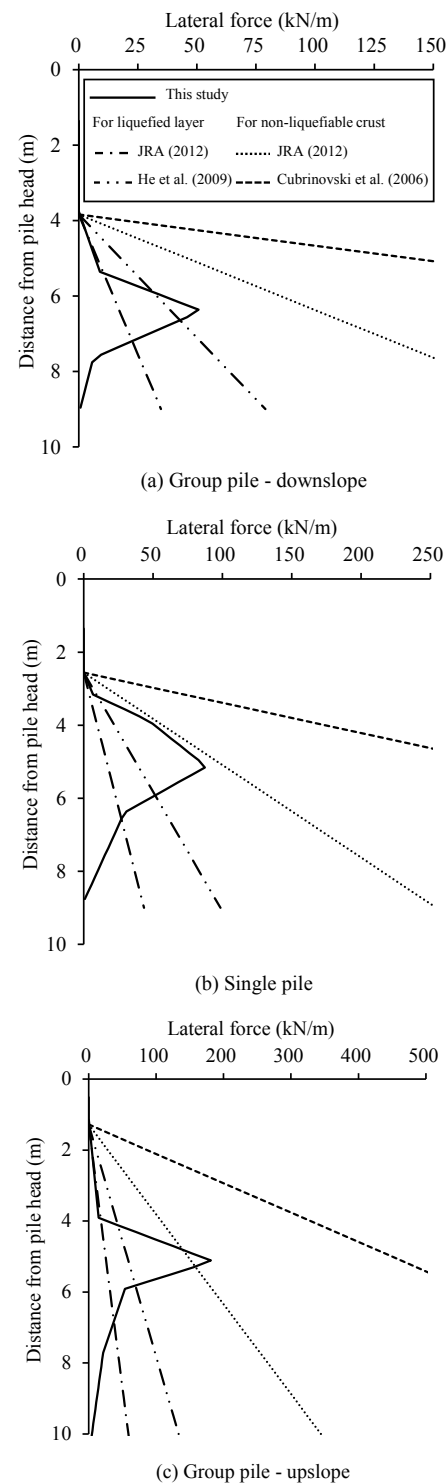


Figure 8. Comparison of experimental lateral force acting on piles obtained from this study and calculated by conventional methods